and deletions, then the current methods would have to be improved in order to make a correct prediction.

ACKNOWLEDGMENTS

I thank Andrew Smellie for helpful discussions in developing these ideas.

REFERENCES

Anfinsen, C. B. (1973) *Science 181*, 223-230.
Bernstein, F. C., Koetzle, T. F., Williams, G. J. B., Meyer, E. F., Brice, M. D., Rodgers, J. R., Kennard, O., Shimanouchi, T., & Tasumi, M. (1977) *J. Mol. Biol. 112*, 535-542.
Bryant, S. H., & Amzel, L. M. (1987) *Int. J. Peptide Protein Res. 29*, 46-52.
Covell, D. G., & Jernigan, R. L. (1990) *Biochemistry 29*, 3287-3294.
Crippen, G. M. (1975) *J. Comput. Phys. 18*, 224-231.
Crippen, G. M., & Snow, M. E. (1990) *Biopolymers 29*, 1479-1489.
Go, N. (1983) *Annu. Rev. Biophys. Bioeng. 12*, 183-210.
Jurs, P. C. (1986) *Computer Software Applications in Chemistry*, pp 198-199, John Wiley and Sons, New York.
Lau, K. F. & Dill, K. A. (1989) *Macromolecules 22*, 3986-3997.
Novotny, J., Rashin, A. A., & Bruccoleri, R. E. (1988) *Proteins: Struct., Funct., Genet. 4*, 19-30.
Seetharamulu, P., & Crippen, G. M. (1991) *J. Math. Chem. 6*, 91-110.
Sippl, M. J. (1990) *J. Mol. Biol. 213*, 859-883.

Contribution to the Thermodynamics of Protein Folding from the Reduction in Water-Accessible Nonpolar Surface Area†

Jeff R. Livingstone,‡ Ruth S. Spolar,§ and M. Thomas Record, Jr.*,‡,§
Departments of Biochemistry and Chemistry, University of Wisconsin—Madison, Madison, Wisconsin 53706
Received October 17, 1990; Revised Manuscript Received January 2, 1991

ABSTRACT: Protein folding and the transfer of hydrocarbons from a dilute aqueous solution to the pure liquid phase are thermodynamically similar in that both processes remove nonpolar surface from water and both are accompanied by anomalously large negative heat capacity changes. On the basis of a limited set of published surface areas, we previously proposed that heat capacity changes (ΔC_p°) for the transfer of hydrocarbons from water to the pure liquid phase and for the folding of globular proteins exhibit the same proportionality to the reduction in water-accessible nonpolar surface area (ΔA_{np}) [Spolar, R. S., Ha, J. H., & Record, M. T., Jr. (1989) *Proc. Natl. Acad. Sci. U.S.A. 86*, 8382-8385]. The consequence of this proposal is that the experimental ΔC_p° for protein folding can be used to obtain estimates of ΔA_{np} and of the contribution to the stability of the folded state from removal of a nonpolar surface from water. In this paper, a rigorous molecular surface area algorithm [Richmond, T. J. (1984) *J. Mol. Biol. 178*, 63-89] is applied to obtain self-consistent values of the water-accessible nonpolar surface areas of the native and completely denatured states of the entire set of globular proteins for which both crystal structures and ΔC_p° of folding have been determined and for the set of liquid and liquefiable hydrocarbons for which ΔC_p° of transfer are known. Both processes (hydrocarbon transfer and protein folding) exhibit the same direct proportionality between ΔC_p° and ΔA_{np}. We conclude that the large negative heat capacity changes observed in protein folding and other self-assembly processes involving proteins provide a quantitative measure of the reduction in the water-accessible nonpolar surface area and of the contribution of the hydrophobic effect to the stability of the native state and to protein assembly.

Noncovalent assembly processes involving proteins, such as folding, oligomerization, and ligand binding, are typically accompanied by large reductions in water-accessible nonpolar surface area. Kauzmann (1959) proposed that the removal of nonpolar amino acid side chains from water (the "hydrophobic effect") should provide a large driving force (ΔG_{hyd}°) for assembly or association processes involving proteins. To quantify the contribution of ΔG_{hyd}° to the observed standard free-energy change (ΔG_{obs}°) for the assembly or association process, most work has focused on analyzing the free energy of transfer (ΔG_{tr}°) of amino acids or their analogues from water to an organic solvent (Cohn & Edsall, 1943; Nozaki & Tanford, 1971; Fauchère & Pliska, 1983) or to the gas phase (Wolfenden et al., 1981). Various hydrophobicity scales have been proposed that rank amino acids according to either their experimental transfer behavior [cf. Cornette et al. (1987)] or their observed distribution in protein crystal structures between the exterior and interior of the folded form (Janin, 1979; Rose et al., 1985a; Miller et al., 1987a). However, a comparison of hydrophobicity scales reveals that, in general, values of ΔG_{tr}° from different scales do not correlate well with each other and that even the relative ranking of amino acids varies from scale to scale (Rose et al., 1985b). Alternatively, the relationship between ΔG_{tr}° of amino acids and the *total* water-accessible surface has been examined (Chothia, 1974) as well as the relationship between ΔG_{tr}° and surface area at the functional group level (Eisenberg & MacLachlan, 1986; Ooi et al., 1987). The use of these relationships to estimate values of ΔG_{hyd}° is complicated by the same problem

† This work was supported in part by NIH Grant GM23467.
* Correspondence should be addressed to this author.
‡ Department of Biochemistry.
§ Department of Chemistry.

0006-2960/91/0430-4237$02.50/0

that gives rise to the current confusing array of hydrophobicity scales: values of ΔG°_{tr} depend not only on the model compound that is transferred but also on the initial and final state of the compound. Consequently any analysis of protein stability based on free energies of transfer of model compounds is limited by assumptions regarding the appropriateness of the model compounds and of the choice of the nonaqueous phase in the transfer process used to model protein folding.

In contrast to the difficulty of unambiguously dissecting ΔG°_{obs} by using ΔG°_{tr}, a simple relationship between changes in heat capacity (ΔC°_p) and water-accessible nonpolar surface area appears to exist for both the transfer of liquid hydrocarbons and the folding of small proteins. [The partial molar heat capacity of hydrocarbons in water, representing the contribution to the heat capacity of the solution per mole of hydrocarbon present, is typically far larger than the molar heat capacity of either the pure hydrocarbon or of water [cf. Tanford (1980) and Cabani et al. (1981)] and demonstrates that the origin of this fundamental thermodynamic effect resides in the hydrocarbon–water interaction.] For the overlapping sets of heat capacity data and estimates of surface area available in the literature, Spolar et al. (1989) observed that values of ΔC°_p for the transfer of hydrocarbons from water to the pure liquid phase and for the folding of four small monomeric proteins exhibit the same proportionality to the reduction in the water-accessible nonpolar surface area. Consequently we proposed that the ΔC°_p associated with folding a polypeptide chain containing both polar and nonpolar surfaces into a compact globular structure is a function only of the reduction in the water-accessible *nonpolar* surface area (ΔA_{np}). The proposed quantitative relationship between ΔC°_p and ΔA_{np} provides a means of estimating the amount of nonpolar surface removed from water in folding proteins for which thermodynamic but not structural data are available. If the liquid hydrocarbon transfer process is the appropriate model system, measurement of ΔC°_p also provides a direct route to estimate the contribution of burial of nonpolar surfaces (ΔG°_{hyd}) to ΔG°_{obs} for processes involving proteins, including protein folding (Sturtevant, 1977; Baldwin, 1986) and site-specific protein–DNA interactions (Ha et al., 1989).

Given the small number of proteins for which nonpolar water-accessible surface areas have been reported and differences in the methods of calculating surface areas of hydrocarbons and proteins in the literature, it is critically important to test the proposed relationship between ΔC°_p and ΔA_{np} by applying a consistent method of calculating surface areas to the set of all proteins and hydrocarbons for which both heat capacity data and structural data are available. In this paper we implement Richmond's exact analytical molecular surface algorithm (Richmond, 1984) to obtain a rigorous and self-consistent measurement of the changes in water-accessible nonpolar surface area in protein folding and liquid hydrocarbon transfer.

Experimental Procedures

Structures. Crystal structures of hydrocarbons that are liquids at 25 °C were obtained directly from the Cambridge Structural Database (CSD), version 4 (Allen et al., 1983). Since structures of ethylbenzene and propylbenzene are not included in the CSD, subsets of atoms from structurally similar molecules were used to represent these compounds. Structures of hydrocarbons that exist as gases at 25 °C were built with the molecular-modeling program MACROMODEL, version 2.5 (Mohamadi et al., 1990), which utilizes the following carbon–carbon bond lengths: aliphatic bond length, 1.54 Å; cyclic bond length, 1.50 Å; aromatic bond length, 1.21 Å. To investigate whether accessible surface areas calculated from these structures are consistent with those calculated from CSD crystal structures, we compared surface areas of the MACROMODEL structures of three representative molecules (benzene, cyclohexane, and hexane) with those obtained from crystal structures. No significant differences were observed.

Table I: van der Waals Radii

atom	set 1 (Å)[a]	set 2 (Å)[b]
tetrahedral carbon	2.0	1.87
trigonal carbon	1.7	1.76
tetrahedral nitrogen	2.0	1.65
trigonal nitrogen	1.7	1.65
tetrahedral oxygen	1.6	1.40
trigonal oxygen	1.5	1.40
sulfhydryl sulfur	2.0	1.85
thioether sulfur	1.8	1.85
Zn^{2+}, Fe^{3+}	0.64	0.64

[a] Richards (1977). [b] Chothia (1976).

Native structures of proteins for which heat capacities of denaturation have been determined (Hawley, 1971; Calderon et al., 1985; Privalov & Gill, 1988; Pace & Laurents, 1989) were chosen from structures in the Brookhaven Protein Data Base (PDB) (Bernstein et al., 1977) for which the resolution is 2.0 Å or less. To model the completely denatured state, extended (β-form) structures were built with MACROMODEL from primary amino acid sequences with completely extended β-form amino acid side-chain configurations. For those proteins containing heme groups (metmyoglobin and ferricytochrome), the water-accessible nonpolar surface area of the heme was calculated separately and added to the water-accessible nonpolar surface area of the corresponding extended chain. Fully extended tripeptide structures of the form Gly-X-Gly for all twenty amino acids were also built with MACROMODEL. The residue side-chain conformations utilized here are from energy-minimized β-form structures (W. C. Still, personal communication) that are similar to those preferred conformations observed in protein crystal structures (Janin et al., 1978; McGregor et al., 1987).

Surface-Area Calculations. Surface-area calculations were performed on a VAXstation 3200 with a modified version of the Richmond ANAREA program (Richmond, 1984).[1] Values and origins of different van der Waals radii used in previous calculations of the total accessible surface area have been tabulated (Richards, 1985). Since previous choices of van der Waals radii for some atoms differ by more than 0.2 Å, it is not surprising that calculations of the total water-accessible surface areas of proteins depend upon the van der Waals radii used (Richards, 1985). We investigated whether this dependence was also observed for our calculations of the *nonpolar* water-accessible surface area (A_{np}). For all structures used to calculate A_{np}, two sets of van der Waals radii were employed: (1) the set adopted by Richards (1977) and used recently, for example, by Rose et al. (1985a) and (2) the set adopted by Chothia (1976) and used recently, for example, by Miller et al. (1987a). Set 1 was derived (with modifications) from the van der Waals radii reported by Bondi (1968), which were obtained from comparisons between electron-density distributions of small inorganic and organic compounds

[1] Our implementation of the Richmond program includes modifications that facilitate the tabulation of the water-accessible areas of each atom and sums of the water-accessible areas of each type of atom in the structure. Contributions from trigonal and tetrahedral carbons are added to obtain the total water-accessible nonpolar surface area of each structure examined.

Table II: Relationship between ΔC_p° and ΔA_{np} for Transfers of Hydrocarbons at 25 °C[a]

	$\Delta C^\circ_{p,w\to g}$[b] (cal mol^{-1} K^{-1})	$\Delta C^\circ_{p,g\to l}$[c] (cal mol^{-1} K^{-1})	$\Delta C^\circ_{p,w\to l}$ (cal mol^{-1} K^{-1})	set 1 radii ΔA_{np} (Å^2)	set 1 radii $\Delta C^\circ_{p,w\to l}/\Delta A_{np}$ (cal mol^{-1} K^{-1} Å^{-2})	set 2 radii ΔA_{np} (Å^2)	set 2 radii $\Delta C^\circ_{p,w\to l}/\Delta A_{np}$ (cal mol^{-1} K^{-1} Å^{-2})
gases							
cyclopropane	−72.4 ± 5.2	7.99	−64.4 ± 4.6	196	−0.329 ± 0.023	183	−0.352 ± 0.025
propane	−76.2 ± 8.8	11.09	−65.2 ± 7.5	207	−0.315 ± 0.036	194	−0.336 ± 0.039
isobutane	−90.1 ± 6.8	10.96	−79.2 ± 6.0	233	−0.340 ± 0.026	219	−0.362 ± 0.027
n-butane	−93.2 ± 8.5	10.61	−82.6 ± 7.5	236	−0.350 ± 0.032	222	−0.372 ± 0.034
1-butene	−93.0 ± 4.6	9.40	−83.6 ± 4.1	214	−0.391 ± 0.019	209	−0.400 ± 0.020
liquids							
cyclohexane			−86.0 ■ 7.2[d]	254	−0.339 ± 0.028	240	−0.358 ± 0.030
n-pentane			−95.6 ± 16.7[d]	266	−0.359 ± 0.063	251	−0.381 ± 0.067
n-hexane			−105.2 ± 10.7[d]	296	−0.355 ± 0.036	279	−0.377 ± 0.038
benzene			−53.8 ± 1.2[d]	212	−0.254 ± 0.006	219	−0.246 ± 0.005
toluene			−62.9 ± 3.1[d]	242	−0.260 ± 0.013	245	−0.257 ± 0.013
ethylbenzene			−76.0 ± 3.1[d]	277	−0.274 ± 0.011	274	−0.277 ± 0.011
propylbenzene			−93.4 ± 6.0[d]	307	−0.304 ± 0.020	304	−0.307 ± 0.020
average					−0.32 ± 0.08		−0.34 ± 0.09
weighted linear least-squares fit (cf. Figure 2)					−0.35 ± 0.08		−0.28 ± 0.08

[a] All error estimates are ±2 SD. [b] Heat capacity change for the transfer from the dilute solution standard state in water to the pure gas phase from Privalov and Gill (1988). Errors estimated from Dec 1984. [c] Heat capacity change for the phase change of the pure solute from the gas phase to the liquid phase, calculated from the data in the TRC Thermodynamic Tables (1984–1989). Error estimates not available. [d] Heat capacity change for the transfer from the dilute solution standard state to the pure liquid phase, from Gill et al. (1976).

and their known packing densities. Set 2 was derived from the packing observed between nonhydrogen atoms in amino acid crystals (Richards, 1985). Radii of set 1 and 2 are shown in Table I. These sets were selected because of their wide use and, in particular, their use by Richards and Chothia, whose studies laid the foundation for calculating protein surface areas.

Results obtained with the Richmond algorithm were checked directly against results obtained with the Richards ACCESS program (Lee & Richards, 1971). When the adjustable slice width (see Discussion) used in the Richards program was set at 0.01 Å, values calculated by the two algorithms agreed to within three significant figures (data not shown). The effect of the choice of slice width has been discussed previously (Richmond & Richards, 1978). However, use of the ACCESS program with a slice width of 0.01 Å consumes ~10 times more CPU time on a VAXstation 3200 than the Richmond algorithm in our calculations of the water-accessible surface areas of the larger proteins studied here.

An additional series of atomic coordinate translation and reformatting programs were written in VAX PASCAL. These programs were used to build linear peptide chains from primary-sequence information in the PDB files, to assign van der Waals radii to atoms in PDB or CSD files, and to reformat PDB or MACROMODEL files into forms suitable for use with the Richmond program. (These programs are available upon request from J.R.L.)

Data Analysis. Data were fit by weighted linear least-squares methods (Press et al., 1986). Reported uncertainties in slopes and intercepts represent two standard deviations from the mean.

RESULTS

Relationship between ΔC_p° and ΔA_{np} for Transfers of Hydrocarbons. Spolar et al. (1989) examined the relationship between the reduction in the water-accessible nonpolar surface area and the heat capacity change for the transfer from water to the pure liquid phase ($\Delta C^\circ_{p,w\to l}$) of those hydrocarbons that exist as liquids at 25 °C. We have extended this data set by including four additional alkanes and one alkene, all of which are in the vapor phase at 25 °C and 1 atm. This requires correcting the observed heat capacity change ($\Delta C^\circ_{p,w\to g}$) for the process of liquifying the hydrocarbon vapor at 25 °C and 1 atm ($\Delta C^\circ_{p,g\to l}$). These data are shown in Table II and represent a virtually complete set of both gaseous and liquid hydrocarbons for which ΔC_p° has been determined. Methane and ethane are omitted in view of the difficulty in estimating $\Delta C^\circ_{p,g\to l}$ for these substances at 25 °C.

Table II also includes values of ΔA_{np} of these hydrocarbons calculated by using the van der Waals radii corresponding to set 1 and set 2. The observed differences in ΔA_{np} demonstrate the sensitivity of the calculation to the choice of radii. The radius for a tetrahedral carbon in set 1 is 6% larger than that in set 2, resulting in approximately 6% larger values of ΔA_{np} for the alkane hydrocarbons when set 1 radii are used. However the radius of a trigonal carbon is 3% smaller in set 1 than in set 2, so that partial compensation at the level of ΔA_{np} occurs for hydrocarbons with both trigonal and tetrahedral carbon atoms. For example, ΔA_{np} for benzene in set 1 is smaller than that in set 2, but ΔA_{np} for propylbenzene in set 1 is larger than that in set 2.

Since it is currently not possible to judge which set of radii is more valid (Richards, 1985), values of ΔA_{np} calculated by using both sets are included in Figure 1, which plots ΔC_p° of transfer of liquid and liquified hydrocarbons as a function of ΔA_{np}. When ΔA_{np} is calculated by using set 1 radii, the plot is linear, with a weighted least-squares slope of −0.35 ± 0.08 cal mol^{-1} K^{-1} Å^{-2} and an intercept of 16 ± 16 cal mol^{-1} K^{-1}. When the van der Waals radii from set 2 are employed, the plot is again linear, with a slope of −0.28 ± 0.08 cal mol^{-1} K^{-1} Å^{-2} and an intercept of 1 ± 18 cal mol^{-1} K^{-1}. Since analysis with either set 1 or set 2 radii yields intercepts that are zero within experimental uncertainty, we conclude that the standard heat capacity change for the transfer process from the dilute solution standard state in water to the pure liquid hydrocarbon is directly proportional to the reduction in the water-accessible nonpolar surface area of the hydrocarbon. This result agrees within experimental uncertainty with that of Gill et al. (1985), who examined the relationship between $\Delta C^\circ_{p,w\to g}$ of 21 nonpolar gases and the estimated number of water molecules in the first hydration shell of these solutes, calculated from the water-accessible nonpolar surface areas by the method of

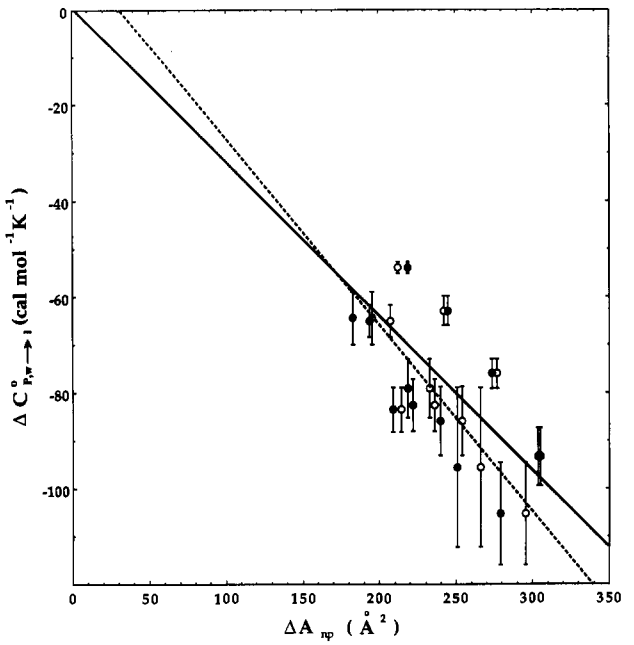

FIGURE 1: Standard heat capacity changes (ΔC_p°) for the process of transferring hydrocarbons to the pure liquid state from the infinitely dilute aqueous solution standard state as a function of the corresponding reduction in their water-accessible nonpolar surface areas (ΔA_{np}). The solid line is the weighted linear least-squares fit obtained by using set 1 radii (○) to calculate ΔA_{np}; the dashed line is the fit obtained by using set 2 radii (●).

Hermann (1972). (We estimate a proportionality of $\Delta C^\circ_{p,w\rightarrow g}/\Delta A_{np} \simeq 0.35$ cal mol^{-1} Å^{-2} from their data.) In retrospect, it is not surprising that the proportionality constant relating the heat capacities of transfer of nonpolar solutes and the water-accessible nonpolar surface is insensitive to the choice of the nonaqueous phase (pure liquid or pure vapor) since these heat capacities of transfer are related by the heat-capacity change accompanying the phase change of the pure solute ($\Delta C^\circ_{p,g\rightarrow l}$). Values of $\Delta C^\circ_{p,g\rightarrow l}$ (cf. Table II) are approximately 10–15% of the corresponding values of $\Delta C^\circ_{p,w\rightarrow l}$ or $\Delta C^\circ_{p,w\rightarrow g}$. This insensitivity of the ΔC_p° of the transfer process of nonpolar solutes to the nature of the nonaqueous phase demonstrates that the anomalous heat capacity effect resides in the interaction between the nonpolar solute and water [cf. Tanford (1980)].

The slopes of the two plots of ΔC_p° vs ΔA_{np} in Figure 1 appear to differ slightly, though the difference is within the uncertainty of the data. In addition, for both sets of radii, a steeper dependence of ΔC_p° on ΔA_{np} is observed for the homologous series of alkylbenzenes than for the aliphatic compounds, presumably as a consequence of the aryl functional group. Since our ultimate goal is to compare the behavior of these model hydrocarbons with that of proteins (see following section) and since both aliphatic and aromatic groups contribute to the nonpolar surface of proteins, we decided at the current level of approximation to treat the aliphatic and aromatic compounds as a single set. This behavior combined with the systematic differences in ΔA_{np} resulting from the choice of van der Waals radii for tetrahedral and trigonal carbons may contribute to the small difference in the slopes obtained in Figure 1 for the different sets of radii. If direct proportionality of ΔC_p° to ΔA_{np} (i.e., a zero intercept) is assumed, $\Delta C_p^\circ = (-0.33 \pm 0.09)\Delta A_{np}$ for either choice of radii (cf. Table II).

Water-Accessible Nonpolar Surface Areas of Proteins: Native and Denatured Forms. The Richmond algorithm was applied to calculate the water-accessible nonpolar surface area of the native and denatured states of all proteins for which both heat capacity data and well-resolved crystal structures are available. Previous studies estimated the surface area of the denatured state by calculating the surface area of each amino acid "X" in an extended (β-form) tripeptide such as Gly-X-Gly or Ala-X-Ala and then summing these contributions over the amino acid composition of the protein (Lee & Richards, 1971; Shrake & Rupley, 1973; Chothia, 1974, 1976; Miller et al., 1987a). We used this procedure and in addition calculated values of A_{np} of the heat-denatured state by modeling the amino acid sequence of the protein as an extended β-form chain, neglecting disulfide cross-links. Both methods effectively model the heat-denatured protein as completely unfolded. However, it has been argued that some residual structure may exist in the denatured form (Howarth & Lian, 1984a,b; Privalov et al., 1989; Bertazzon et al., 1990). Our calculation yields the *maximum* water-accessible nonpolar surface area of the denatured state.

Table III: Water-Accessible Nonpolar Surface Area of Amino Acid X in Gly-X-Gly

amino acid	set 1 (Å^2)[a]	set 2 (Å^2)[b]
Ala	80.4	77.1
Arg	84.5	91.4
Asn	41.9	49.1
Asp	48.9	51.9
Cys	47.3	47.2
Gln	47.3	60.2
Glu	57.0	63.2
Gly	45.9	44.6
His	99.1	107.2
Ile	154.0	148.2
Leu	156.0	150.3
Lys	109.3	121.4
Met	125.0	118.4
Phe	168.4	173.3
Pro	127.0	121.5
Ser	57.4	57.6
Thr	88.7	87.2
Trp	177.2	185.7
Tyr	137.4	144.7
Val	127.1	122.1

[a] Richards (1977). [b] Chothia (1976).

To compare nonpolar surface areas calculated using the extended β-form chain with those calculated from Gly-X-Gly tripeptides, we first applied the Richmond algorithm to calculate the nonpolar surface areas of the twenty amino acid residues in the fully extended β-form of Gly-X-Gly. Values obtained with the alternative choices of van der Waals radii are shown in Table III. Amino acid side chains composed entirely of aliphatic carbons exhibit the same trend as the hydrocarbons; values of A_{np} calculated with set 1 radii are greater due to the larger radius of the tetrahedral carbon in set 1. However, differences between values of A_{np} of side chains composed of both carbon and polar atoms depend not only on the differences between the carbon radii of the two sets but also on the differences between the polar radii. When the accessibility of the nonpolar surface is calculated, polar atoms block adjacent carbons from van der Waals contact with water. Since the radii of polar atoms in set 1 are larger than those in set 2, they occlude more nonpolar surface. Consequently, values of A_{np} for mixed-atom side chains in set 1 are generally smaller than those in set 2. Examples of this effect are given by lysine and glutamate, both of which have side chains ending in polar atoms that limit the accessibility of the interior carbon atoms. Figure 2 plots the values of A_{np} given by tripeptide summation versus those calculated for the actual (contiguous) chain and shows that the results of the two methods of estimating the nonpolar surface area are propor-

Table IV: Relationship between ΔC_p° and ΔA_{np} for Protein Folding

		set 1 radii			set 2 radii		
protein	file[a]	$A_{np,den}$ ($\times 10^3$ Å^2)	$A_{np,nat}$ ($\times 10^3$ Å^2)	$\Delta C^\circ_{p,fold}/\Delta A_{np}$[b] (cal mol^{-1} K^{-1} Å^{-2})	$A_{np,den}$ ($\times 10^3$ Å^2)	$A_{np,nat}$ ($\times 10^3$ Å^2)	$\Delta C^\circ_{p,fold}/\Delta A_{np}$[b] (cal mol^{-1} K^{-1} Å^{-2})
trypsin inhibitor	5PTI	4.68	2.03	−0.272 ± 0.042	4.84	2.15	−0.268 ± 0.044
parvalbumin B	3CPV	9.31	3.82	−0.200 ± 0.018	9.53	4.08	−0.202 ± 0.018
ribonuclease A	1RN3	9.34	3.53	−0.212 ± 0.031	9.80	3.86	−0.207 ± 0.030
lysozyme	1LZT	9.92	3.05	−0.224 ± 0.035	10.4	3.41	−0.220 ± 0.034
ribonuclease T_1	2RNT	7.76	2.60	−0.320 ± 0.032[c]	8.08	2.74	−0.301 ± 0.031[c]
ferricytochrome	1CYC	9.20	3.65	−0.311 ± 0.046	9.62	4.00	−0.308 ± 0.046
staph. nuclease	2SNS	12.6	4.71	−0.285 ± 0.011[d]	13.2	5.19	−0.281 ± 0.011[d]
metmyoglobin	4MBN	14.2	4.49	−0.285 ± 0.043	14.9	5.03	−0.281 ± 0.043
β-trypsin	2PTN	16.4	4.60	−0.242 ± 0.038	18.6	4.96	−0.209 ± 0.033
papain	9PAP	17.2	4.45	−0.228 ± 0.035	17.9	4.90	−0.225 ± 0.035
α-chymotrypsin	5CHA	19.9	5.16	−0.205 ± 0.031	20.4	5.45	−0.203 ± 0.031
chymotrypsinogen	2CGA	20.2	5.62	−0.260 ± 0.018[e]	20.6	6.04	−0.260 ± 0.018[e]
carbonic anhydrase	2CAB	21.4	5.68	−0.243 ± 0.037	22.4	6.28	−0.237 ± 0.036
pepsinogen	1PSG	31.3	7.59	−0.257 ± 0.039	31.8	8.05	−0.257 ± 0.039
weighted linear least-squares fit				−0.25 ± 0.02			−0.25 ± 0.02

[a] File name in the Protein Data Bank. [b] All heat capacity data are from Privalov and Gill (1988) unless otherwise noted. Values of $\Delta C^\circ_{p,fold}$ from Privalov and Gill are reported at 50 °C. [c] Pace and Laurents (1989). Value of $\Delta C^\circ_{p,fold}$ reported at 25 °C. [d] Calderon et al. (1985). Value of $\Delta C^\circ_{p,fold}$ reported at 53 °C. [e] Hawley (1971). Value of $\Delta C^\circ_{p,fold}$ reported at 0 °C.

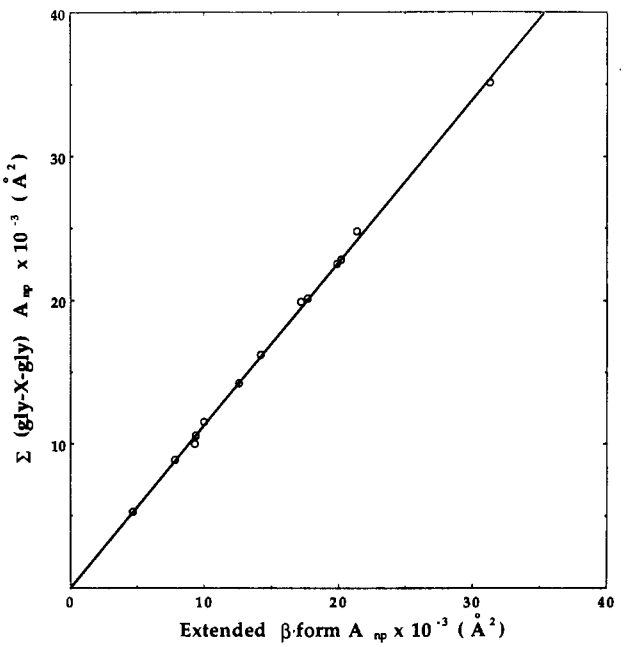

FIGURE 2: Comparison of the values of A_{np} of the unfolded polypeptide chain calculated by summation of contributions from central residues of β-form tripeptides [Σ(Gly-X-Gly)] and from the extended β-form polypeptide chain. The line is the linear least-squares fit and corresponds to the equation $y = (1.15 \pm 0.01)x - (185 \pm 388)$.

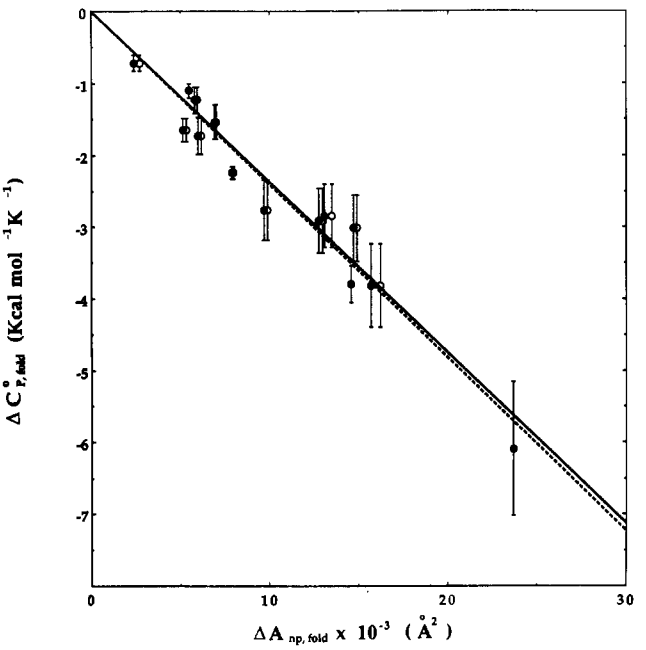

FIGURE 3: Standard heat capacity changes ($\Delta C^\circ_{p,fold}$) for the process of protein folding as a function of the reduction in water-accessible nonpolar surface area accompanying folding (ΔA_{np}). The denatured state is assumed to be in the extended β-form. The solid line is the weighted least-squares fit obtained by using set 1 radii (○) to calculate ΔA_{np}; the dashed line is the fit obtained by using set 2 radii (●). Where the two values of ΔA_{np} agree within the size of the data point, only one point (●) is plotted.

tional to one another. Values of A_{np} determined by summation of tripeptides are approximately 15% larger than those determined by using the actual polypeptide chain, independent of which set of van der Waals radii is used. In what follows, we use the extended polypeptide chain to calculate A_{np} for the denatured state of proteins ($A_{np,den}$).

Relationship between ΔC_p° and ΔA_{np} for Protein Folding. Table IV compiles the amounts of water-accessible nonpolar surface in the denatured ($A_{np,den}$) and the native ($A_{np,nat}$) states and the ratio of $\Delta C^\circ_{p,fold}$ to the reduction in the water-accessible nonpolar surface area upon folding (ΔA_{np}) for both sets of van der Waals radii. These data are shown in Figure 3, which plots $\Delta C^\circ_{p,fold}$ versus ΔA_{np} calculated by using radii from either set 1 or set 2. Both sets of radii yield linear plots. A weighted linear least-squares fit of the data when set 1 radii are used yields a slope of −0.25 ± 0.03 cal mol^{-1} K^{-1} Å^{-2} and an intercept of −7 ± 220 cal mol^{-1} K^{-1}. The fit of the data when set 2 radii are used gives a slope of −0.25 ± 0.03 cal mol^{-1} K^{-1} Å^{-2} and an intercept of 1 ± 220 cal mol^{-1} K^{-1}. (The same slope and intercept within experimental uncertainty are obtained if the denatured state is also modeled as having some residual structure that buries up to 30% of the nonpolar surface which is water-accessible in the extended β-form polypeptide chain.) Thus within experimental error the heat capacity change for protein folding is directly proportional to ΔA_{np} and exhibits the same proportionality as that found for the liquid hydrocarbon transfer data, independent of the choice of van der Waals radii used.

A graphic demonstration of the congruence between heat capacity changes of transfers of nonpolar solutes from water and of protein folding is provided by the log–log plot of Figure

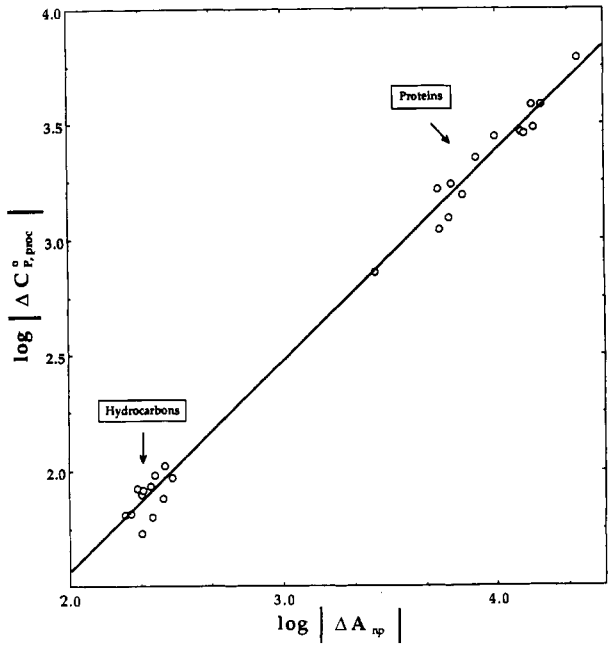

FIGURE 4: Log–log plot of ΔC_p° vs ΔA_{np} for the processes of hydrocarbon transfer (Table II) and protein folding (Table IV), demonstrating the congruence of the two data sets.

4 in which these two sets of heat capacity data are compared as a function of ΔA_{np}. On the scale of this plot, differences in ΔA_{np} resulting from the alternative choices of van der Waals radii are insignificant. Clearly the hydrocarbon and protein data, which cover very different ranges of magnitudes of ΔC_p° and ΔA_{np}, lie on a common line. The slope of this line is unity within experimental error (0.98 ± 0.02) and demonstrates the direct proportionality between ΔC_p° and ΔA_{np} for the composite data set. The intercept, which yields the relationship $\Delta C_p^\circ = (-0.32 \pm 0.03)\Delta A_{np}$, is in good agreement with the individual analyses of the hydrocarbon and protein data. (If one assumes exact congruence between the liquid hydrocarbon and protein data sets by fixing the slope of this plot at unity, the resulting intercept is within experimental uncertainty of the one stated above.) We conclude from this result that the primary origin of the large negative heat capacity change in protein folding is the large reduction in the water-accessible nonpolar surface during the folding process.

Discussion

Calculation of the Water-Accessible Nonpolar Surface Area. In their classic paper, Lee and Richards (1971) developed an algorithm to estimate the "water-accessible surface area" of a protein, given the coordinates of its individual atoms. This area is measured by taking planar slices through a three-dimensional X-ray crystal structure at defined intervals and measuring the sum of the exterior arcs of all atoms bisected by the plane. The resultant sum is multiplied by the width of the plane, and the totals of all products are summed to determine the total accessible surface of the protein. The Lee and Richards (1971) program ACCESS, which implements this algorithm, reports water-accessible surface areas only in terms of component atoms. Hence, it is necessary to scan through the output by hand and sum the surface areas of those atoms that have been selected for analysis. Some atoms line the inside surface of obviously non-water-accessible cavities or pockets. However, in their reported results, these areas were found to be less than 1% of the total accessible surface of all proteins studied. This is consistent with more recent examinations of the locations of water molecules in protein crystal structures (Edsall & McKenzie, 1983; Rashin et al., 1986; Saenger, 1987; Goodfellow et al., 1989).

Using the same definition of accessible surface, Shrake and Rupley (1973) generated an alternative algorithm to calculate accessible surface areas based upon the placement of a set of dots at a known density across the spherical hydrated surface of each atom in a protein crystal structure. All dots that lay in the interior of other overlapping hydrated van der Waals shells are turned off, and the remaining dots are summed. Since the surface density of the dots is predefined, a ratio of the number of remaining dots divided by the dot density provides an estimate of the total water-accessible surface area of the protein. This algorithm has been implemented by Chothia and others to estimate water-accessible surface areas of monomeric and oligomeric proteins over a wide range of molecular weights (Lesk et al., 1985; Miller et al., 1987a,b; Janin et al., 1988).

Using the Richards (1977) definition of accessible surface, Richmond (1984) developed an exact analytical algorithm that measures the amount of surface area exterior to an arbitrary number of overlapping spheres. This algorithm is based upon the use of a special case of the Gauss–Bonnet theorem from differential geometry. This algorithm was originally used to investigate relationships between the volume excluded to solvent and the pair-wise interaction free energies of molecules in solution (Richmond, 1984). We have implemented this algorithm in order to determine the water-accessible nonpolar surface areas of simple hydrocarbon molecules, folded and unfolded forms of proteins, and Gly-X-Gly tripeptide structures. Using the Richmond analytical algorithm with a consistent set of van der Waals radii for all of these structures, we obtain absolute and relative water-accessible nonpolar surface areas that should be more accurate and more self-consistent than those previously available. For the hydrocarbons in Table II, values of ΔA_{np} calculated with either set of van der Waals radii (and a 1.4-Å probe radius) by the Richmond (1984) algorithm are approximately 10% smaller than those reported by Hermann (1972), who used a 1.5-Å probe radius. For the four proteins considered by Spolar et al. (1989), our calculated values of the water-accessible nonpolar surface areas of the denatured and native states and of ΔA_{np} are approximately 5–20% smaller than those previously reported, depending on the radii set used.

Liquid Hydrocarbon Transfer as a Model of Protein Folding. Given the complexity of the process of folding a linear polypeptide chain into a compact three-dimensional structure, phase-transfer studies with model compounds have been proposed as a means of isolating various aspects of the folding process and thereby providing insight into the interactions responsible for the stability of the native state. In particular, Kauzmann (1959) proposed that the transfer of hydrocarbons from water to a nonaqueous phase modeled the contribution to protein stability from the removal of nonpolar side chains from water. Calorimetric studies used to decompose ΔG_{tr}° into its enthalpic and entropic contributions demonstrate the existence of very large negative heat capacity changes in the transfer of hydrocarbons and other model compounds from water to a nonaqueous phase (Gill et al., 1976; Dec, 1984; Olofsson et al., 1984; Naghibi et al., 1986, 1987; Murphy & Gill, 1989a,b). This large negative ΔC_p° is a fundamental thermodynamic characteristic of the transfer of hydrocarbons from water and gives rise to the unique thermodynamic behavior defined as the "hydrophobic effect" [cf. Tanford (1980), Ha et al. (1989), Muller (1990), Dill (1990), and references therein]. [Changes in enthalpy (ΔH°)

and entropy ($\Delta S°$) upon transfer are strong functions of temperature as a direct result of the large negative ΔC_p° and hence are less fundamental indicators of the hydrophobic effect when determined at only one temperature.] Calorimetric studies also demonstrate the existence of a very large negative ΔC_p° in the process of folding globular proteins [cf. Privalov (1979, 1989) for reviews]. Since both processes remove the nonpolar surface from contact with water, one test of whether the thermodynamics of transfer of the nonpolar surface are an important component of the thermodynamics of folding is to determine whether relationships observed between ΔC_p° of transfer and ΔA_{np} for gases (Gill et al., 1985) and liquids (Spolar et al., 1989) also exist for protein folding. Figures 3 and 4 demonstrate that the constant of proportionality between ΔC_p° and ΔA_{np} for protein folding is the same as that for the transfer of hydrocarbons from water to the pure liquid phase. In addition, since the fit of the protein data yields an intercept that is zero within experimental uncertainty, we conclude that the removal of the nonpolar surface from water dominates the ΔC_p° of protein folding.

Since the heat capacity effects for hydrocarbon transfer and protein folding have generally been investigated over different temperature ranges, the above conclusion is based on the assumption that the measured heat capacity changes for these processes are not significant functions of temperature. To date, most analyses of the role of ΔC_p° in processes involving proteins or model nonpolar solutes have employed this assumption [cf. e.g., Sturtevant (1977), Baldwin (1986), Privalov and Gill (1988), and Murphy et al. (1990)]. Privalov et al. (1989) recently observed that heat capacity changes for the folding of three proteins (myoglobin, lysozyme, and RNase A) are relatively temperature-independent over the temperature range of 0–50 °C. Transfers of benzene and toluene from water to the pure liquid phase (Makhatadze & Privalov, 1988) and transfers of methane, ethane, and propane from water to the gas phase (Nagahibi et al., 1986, 1987) exhibit somewhat temperature-dependent changes in heat capacity. The rate of change of $\Delta C_{p,tr}^\circ$ with temperature ($d\Delta C_{p,tr}^\circ/dT$) between 0 and 50 °C is similar for all these hydrocarbon transfer processes. From the published data, we estimate that $d\Delta C_{p,tr}^\circ/dT \simeq 0.24$ cal mol^{-1} K^{-2}. If we assume that this value of $d\Delta C_p^\circ/dT$ is generally applicable to the hydrocarbon data discussed here (Table II), then this translates into a maximum change in $\Delta C_{p,w\rightarrow l}^\circ$ from the values given at 25 °C of approximately 6.1 cal mol^{-1} K^{-1} as the temperature is varied from 0 to 50 °C. If indeed all hydrocarbons in Table II exhibit similar temperature dependences of $\Delta C_{p,tr}^\circ$, then only the intercept and not the slope of the linear relationship shown in Figure 1 would be affected by inclusion of this effect. A 6.1 cal mol^{-1} K^{-1} change in the intercept is within the reported error of the intercept at 25 °C. Consequently, use of a temperature-independent $\Delta C_{p,tr}^\circ$ does *not* affect the conclusion that the hydrophobic effect is the dominant contributor to $\Delta C_{p,fold}^\circ$.

The direct proportionality of $\Delta C_{p,fold}^\circ$ to ΔA_{np} is striking since Sturtevant's (1977) examination of possible origins of the heat capacity changes observed to accompany protein folding and ligand binding suggested that, in addition to the hydrophobic effect, changes in vibrational modes and temperature-dependent shifts in equilibria between multiple conformations of either the native or denatured state could also contribute to ΔC_p°. Demonstration that the liquid hydrocarbon transfer process models protein folding at the level of ΔC_p° verifies one of the principal assumptions in application of the liquid hydrocarbon transfer data to estimate the contribution of the hydrophobic effect (ΔG_{hyd}°) to the overall free-energy change for protein folding from the observed ΔC_p° of folding (Sturtevant, 1977; Baldwin, 1986; Spolar et al., 1989). Ha et al. (1989) have applied a parallel analysis to interpret the large negative ΔC_p° of site-specific protein–DNA interactions in terms of removal of the nonpolar surface from water and its contribution to the standard free energy of binding. The hydrophobic driving force (i.e., the removal of the nonpolar surface from water) appears to contribute $>10^2$ kcal mol^{-1} of free energy to the stability of typical globular proteins, protein assemblies, and site-specific protein–DNA interactions (Sturtevant, 1977; Baldwin, 1986; Spolar et al., 1989; Ha et al., 1989). While the numerical uncertainty in this result is presently still large, the major role of the hydrophobic effect in these processes seems clear.

Conclusion. We have used the rigorous Richmond (1984) algorithm and two plausible sets of van der Waals radii to demonstrate that the ΔC_p° of protein folding (1) is directly proportional to the reduction in the water-accessible nonpolar surface area ΔA_{np} and (2) exhibits the same proportionality to ΔA_{np} as that found for the transfer of hydrocarbons from the dilute aqueous solution standard state to the pure liquid state. We conclude that the ΔC_p° of protein folding is dominated by the hydrophobic effect. Experimental determinations of ΔC_p° can therefore be used to quantify the amount of nonpolar surface removed from water upon folding and the contribution of the hydrophobic driving force to protein stability and other noncovalent self-assembly processes.

Acknowledgments

We thank Dr. T. J. Richmond for generously providing us with the source code of his ANAREA program; Drs. J. W. Robbin, T. J. Richmond, and M. L. Connolly for extremely helpful and insightful discussions regarding the geometrical complexities of the ANAREA algorithm; Dr. C. N. Pace for providing us with the ACCESS program and the crystal structure coordinates for ribonuclease T_1; Dr. W. C. Still for help with the MACROMODEL program; Craig Bingman, Dr. A. Pathiaseril, and Dr. D. H. Rich for assistance in securing the necessary PDB files; Drs. S. H. Gellman, F. M. Richards, J. D. Ferry, A. F. Shrake, and members of the Record laboratory for their suggestions and comments on the manuscript; and Sheila Aiello for help with preparation of the manuscript.

Registry No. Cyclopropane, 75-19-4; propane, 74-98-6; isobutane, 75-28-5; *n*-butane, 106-97-8; 1-butene, 106-98-9; *n*-pentane, 109-66-0; *n*-hexane, 110-54-3; toluene, 108-88-3; ethylbenzene, 100-41-4; propylbenzene, 103-65-1; trypsin inhibitor, 9035-81-8; ribonuclease A, 9001-99-4; lysozyme, 9001-63-2; ribonuclease T_1, 9026-12-4; nuclease, 9026-81-7; β-trypsin, 9002-07-7; papain, 9001-73-4; α-chymotrypsin, 9004-07-3; chymotrypsinogen, 9035-75-0; carbonic anhydrase, 9001-03-0; pepsinogen, 9001-10-9.

References

Allen, F. H., Kennard, O., & Taylor, R. (1983) *Acc. Chem. Res. 16*, 146–153.

Baldwin, R. L. (1986) *Proc. Natl. Acad. Sci. U.S.A. 83*, 8069–8072.

Bernstein, F. C., Koetzle, T. F., Williams, G. J. B., Meyer, E. F., Jr., Brice, M. D., Rodgers, J. R., Kennard, O., Shimanouchi, T., & Tasumi, M. (1977) *J. Mol. Biol. 112*, 535–542.

Bertazzon, A., Tian, G. H., Lamblin, A., & Tsong, T. Y. (1990) *Biochemistry 29*, 291–298.

Bondi, A. (1968) *Physical Properties of Molecular Crystals, Liquids and Glasses*, Chapter 14, Wiley, New York.

Cabani, S., Gianni, P., Mollica, V., & Lepori, L. (1981) *J. Solution Chem. 10*, 563–591.

Calderon, R. O., Stolowich, N. J., Gerlt, J. A., & Sturtevant, J. M. (1985) *Biochemistry 24*, 6044–6049.
Chothia, C. (1974) *Nature 248*, 338–339.
Chothia, C. (1976) *J. Mol. Biol. 105*, 1–14.
Cohn, E. J., & Edsall, J. T. (1943) *Proteins, Amino Acids, and Peptides as Ions and Dipolar Ions*, Chapter 9, Van Nostrand-Reinhold, Princeton.
Cornette, J. L., Cease, K. B., Margalit, H., Spouge, J. L., Berzofsky, J. A., & DeLisi, C. (1987) *J. Mol. Biol. 195*, 659–685.
Dec, S. F. (1984) Ph.D. Thesis, University of Colorado at Boulder, Boulder, Colorado.
Dill, K. A. (1990) *Biochemistry 29*, 7133–7155.
Edsall, J. T., & McKenzie, H. A. (1983) *Adv. Biophys. 16*, 53–183.
Eisenberg, D., & McLachlan, A. D. (1986) *Nature 319*, 199–203.
Fauchère, J.-L., & Pliska, V. (1983) *Eur. J. Med. Chem. 18*, 369–375.
Gill, S. J., Nichols, N. F., & Wadsö, I. (1976) *J. Chem. Thermodyn. 8*, 445–452.
Gill, S. J., Dec, S. F., Olofsson, G., & Wadsö, I. (1985) *J. Phys. Chem. 89*, 3758–3761.
Goodfellow, J. M., Thanki, N., & Thornton, J. M. (1989) *Mol. Simul. 3*, 167–182.
Ha, J. H., Spolar, R. S., & Record, M. T., Jr. (1989) *J. Mol. Biol. 209*, 801–816.
Hawley, S. A. (1971) *Biochemistry 10*, 2436–2442.
Hermann, R. B. (1972) *J. Phys. Chem. 76*, 2754–2759.
Howarth, O. W., & Lian, L. Y. (1984a) *Biochemistry 23*, 3515–3521.
Howarth, O. W., & Lian, L. Y. (1984b) *Biochemistry 23*, 3522–3526.
Janin, J. (1979) *Nature 277*, 491–492.
Janin, J., Wodak, S., Levitt, M., & Maigret, B. (1978) *J. Mol. Biol. 125*, 357–386.
Janin, J., Miller, S., & Chothia, C. (1988) *J. Mol. Biol. 204*, 155–164.
Kauzmann, W. (1959) *Adv. Protein Chem. 14*, 1–63.
Lee, B., & Richards, F. M. (1971) *J. Mol. Biol. 55*, 379–400.
Lesk, A. M., Janin, J., Wodak, S., & Chothia, C. (1985) *J. Mol. Biol. 183*, 267–270.
McGregor, M. J., Islam, S. A., & Sternberg, M. J. E. (1987) *J. Mol. Biol. 198*, 295–310.
Makhatadze, G. I., & Privalov, P. L. (1988) *J. Chem. Thermodyn. 20*, 405–412.
Miller, S., Janin, J., Lesk, A. M., & Chothia, C. (1987a) *J. Mol. Biol. 196*, 641–656.
Miller, S., Lesk, A. M., Janin, J., & Chothia, C. (1987b) *Nature 328*, 834–836.
Mohamadi, F., Richards, N. G. J., Guida, W. C., Liskamp, R., Lipton, M., Caufield, C., Chang, G., Hendrickson, T., & Still, W. C. (1990) *J. Comput. Chem. 11*, 440–467.
Muller, N. (1990) *Acc. Chem. Res. 23*, 23–28.
Murphy, K. P., & Gill, S. J. (1989a) *J. Chem. Thermodyn. 21*, 903–913.
Murphy, K. P., & Gill, S. J. (1989b) *Thermochim. Acta 139*, 279–290.
Murphy, K. P., Privalov, P. L., & Gill, S. J. (1990) *Science 247*, 559–561.
Naghibi, H., Dec, S. F., & Gill, S. J. (1986) *J. Phys. Chem. 90*, 4621–4623.
Naghibi, H., Dec, S. F., & Gill, S. J. (1987) *J. Phys. Chem. 91*, 245–248.
Nozaki, Y., & Tanford, C. (1971) *J. Biol. Chem. 246*, 2211–2217.
Olofsson, G., Oshodj, A. A., Qvarnström, E., & Wadsö, I. (1984) *J. Chem. Thermodyn. 16*, 1041–1052.
Ooi, T., Oobatake, M., Nēmethy, G., & Scheraga, H. A. (1987) *Proc. Natl. Acad. Sci. U.S.A. 84*, 3086–3090.
Pace, C. N., & Laurents, D. V. (1989) *Biochemistry 28*, 2520–2525.
Press, W. H., Flannery, B. P., Teukolsky, S. A., & Vetterling, W. T. (1986) *Numerical Recipes: The Art of Scientific Computing*, Chapter 14, Cambridge University Press, Cambridge.
Privalov, P. L. (1979) *Adv. Protein Chem. 33*, 167–241.
Privalov, P. L. (1989) *Annu. Rev. Biophys. Biophys. Chem. 18*, 47–69.
Privalov, P. L., & Gill, S. J. (1988) *Adv. Protein Chem. 39*, 191–234.
Privalov, P. L., Tiktopulo, E. I., Venyaminov, S. Y., Griko, Y. V., Makhatadze, G. I., & Khechinashvili, N. N. (1989) *J. Mol. Biol. 205*, 737–750.
Rashin, A. A., Iofin, M., & Honig, B. (1986) *Biochemistry 25*, 3619–3625.
Richards, F. M. (1977) *Annu. Rev. Biophys. Bioeng. 6*, 151–176.
Richards, F. M. (1985) *Methods Enzymol. 115*, 440–464.
Richmond, T. J. (1984) *J. Mol. Biol. 178*, 63–89.
Richmond, T. J., & Richards, F. M. (1978) *J. Mol. Biol. 119*, 537–555.
Rose, G. D., Geselowitz, A. R., Lesser, G. J., Lee, R. H., & Zehfus, M. H. (1985a) *Science 229*, 834–838.
Rose, G. D., Gierasch, L. M., & Smith, J. A. (1985b) *Adv. Protein Chem. 37*, 1–109.
Saenger, W. (1987) *Annu. Rev. Biophys. Chem. 16*, 93–114.
Shrake, A., & Rupley, J. A. (1973) *J. Mol. Biol. 79*, 351–371.
Spolar, R. S., Ha., J. H., & Record, M. T., Jr. (1989) *Proc. Natl. Acad. Sci. U.S.A. 86*, 8382–8385.
Sturtevant, J. M. (1977) *Proc. Natl. Acad. Sci. U.S.A. 74*, 2236–2240.
Tanford, C. (1980) *The Hydrophobic Effect: Formation of Micelles and Biological Membranes*, John Wiley and Sons, New York.
TRC Thermodynamic Tables—Hydrocarbons (1984–1989) Thermodynamic Research Center, The Texas A&M University System, College Station, Texas [Loose-leaf data sheets p 1010 (1984); p 1350 (1985); p 1970 (1989); p 2600 (1988)].
Wolfenden, R., Andersson, L., Cullis, P. M., & Southgate, C. C. B. (1981) *Biochemistry 20*, 849–855.